

# PHYSICAL REVIEW C

## NUCLEAR PHYSICS

THIRD SERIES, VOL. 6, No. 2

August 1972

### Rescattering Effects in the ${}^2\text{H}(p, 2p)n$ and ${}^2\text{H}(p, pn)n$ Reactions Induced by 20- to 60-MeV Protons

J. L. Durand, J. Arvieux, A. Fiore, C. Perrin, and M. Durand  
*Institut des Sciences Nucléaires, Grenoble 38, France*  
(Received 16 March 1972)

The  $(p, p)$  and  $(n, p)$  quasifree scattering have been studied in the same experiment. The data are compared with single-scattering models and with calculations of the rescattering series up to the third order. Single-scattering calculations give the shape of the spectra, but there is a discrepancy between calculated and experimental absolute values of the cross sections. Calculations of the rescattering effect do not converge below 20 MeV but reproduce both the magnitude and the shape of the quasifree peak above 40 MeV.

#### I. INTRODUCTION

We consider the three-body reaction  ${}^2\text{H}(p, 123)$ , where deuterons are broken by incident protons. We are dealing especially with the mechanism in which the nucleons 1 and 2 engage in quasifree scattering (QFS), the particle 3 being only a "spectator." The differential cross section  $\sigma(E_1, \Omega_1, \Omega_2)$  plotted against  $E_1$ , the energy of particle 1, shows a strong enhancement when the momentum transferred to particle 3 approaches zero. This feature appears for energies as low as 7 MeV,<sup>1,2</sup> although the wavelength associated with the incident particle is large compared to the deuteron size. The cross sections calculated by simple QFS models<sup>1-9</sup> generally reproduce well the shape of the experimental spectra, but the absolute values disagree, the agreement being better when the energy increases. For example, for the  $(p, 2p)$  reaction  $\sigma_{\text{ex}}/\sigma_{\text{th}} = 0.20$  at 10 MeV<sup>2</sup> and 0.83 at 198 MeV.<sup>9</sup> It is thought that this disagreement is principally produced by two effects usually neglected in the calculations; namely, the rescattering effects and the failure to consider off-shell interactions. The relative importance of these two effects varies with the energy; the rescattering terms are very important at low

energy,<sup>10</sup> but the off-shell effects are practically unknown.

We report here a systematic experimental study of the  $p$ - $p$  and  $n$ - $p$  QFS in the reactions  ${}^2\text{H}(p, 2p)$  and  ${}^2\text{H}(p, pn)$  in the energy range 20 to 60 MeV. The purpose of this experiment is: (1) to study the QFS mechanism in the intermediate-energy region as a function of the incident proton energy and (2) to compare for the same mechanism different types of nucleon-nucleon interactions. Data are compared with diverse types of direct interactions, and the effect of rescattering terms up to the third order are considered.

#### II. EXPERIMENTAL SETUP

The proton beam of the variable energy cyclotron of Grenoble impinges upon a  $\text{CD}_2$  target of 4.0 or 2.0 mg/cm<sup>2</sup> in a spherical scattering chamber where counters can be set in the entire  $4\pi$  sr space.<sup>11</sup> The two interacting particles are detected in coincidence in a symmetrical arrangement relative to the incident beam. The angle of QFS is a function<sup>12</sup> of the incident energy and it is of the order of 42.5 to 43° between 20 and 60 MeV.

Proton telescopes are composed of  $\Delta E$  surface-barrier detectors of 200- $\mu\text{m}$  thickness and  $E$  de-

tectors which were either 4-mm- or 2-4-mm-thick Si(Li) detectors stacked together. The neutron detector is made of NE 213 liquid scintillator optically coupled to a XP 1021 photomultiplier. In most cases the  $n$ - $p$  interaction has been studied in the same experiment as the  $p$ - $p$  interaction. The  ${}^2\text{H}(p, 2p)$  reaction takes place in the horizontal plane and the  ${}^2\text{H}(p, pn)$  reaction in a plane making an angle of  $40^\circ$  with the preceding one. The simplified electronics system is shown Fig. 1(a) for the  ${}^2\text{H}(p, 2p)$  and Fig. 1(b) for the  ${}^2\text{H}(p, pn)$  experiment.

The following eight variables defining the detected events are recorded on line on a magnetic tape driven by a PDP-9 computer. For the reaction  ${}^2\text{H}(p, p_1p_2)$  they are:  $E_1$  and  $\Delta E_1$ , the energy and energy loss of proton 1;  $E_2$  and  $\Delta E_2$ , the same for proton 2; and  $\Delta t$  the time interval between the detections of proton 1 and 2. For the  ${}^2\text{H}(p, pn)$  reaction they are:  $E_p$  and  $\Delta E_p$ , the energy and energy loss of the proton; and the difference in time of flight, TOF, between the proton and the neutron. An example of the time spectrum given by the time-to-amplitude converter (TAC) for the  ${}^2\text{H}(p, p_1p_2)$  experiment is given in Fig. 2. One observes three peaks separated by 65.2 nsec, the period of

the cyclotron at 40 MeV, corresponding to three consecutive bursts of the cyclotron. The first peak contains true and random coincident events, the second and third peaks contain random events only. These two peaks have the same amplitude, which indicates that there is no modulation of the cyclotron bursts. The rejection of the random coincidences is done by subtracting in the  $E_1$ - $E_2$  plane the events corresponding to one of these last two peaks from the spectrum corresponding to the first peak. The treatment of the data is computed off line. Particle identification is done by selecting the proper particle in the  $E$ - $\Delta E$  spectrum. During data acquisition an interface permits visualization of two of the variables defined above on a biparametric Tridac Intertechnique 4096-channel analyzer. Figures 3(a) and 3(b) show, respectively, typical biparametric displays of events in the  $(E_1, E_2)$  plane for the  ${}^2\text{H}(p, p_1p_2)$  reaction and in the  $(E_p, \text{TOF})$  plane for the  ${}^2\text{H}(p, pn)$  reaction. Energy calibration is done by means of the  ${}^{12}\text{C}(p, p')$ ,  ${}^2\text{H}(p, p)$ ,  ${}^2\text{H}(p, d)$ , and  $\text{H}(p, p)$  reaction kinematics. The average over-all energy resolution is of the order of 150 to 250 keV and the time resolution is 2.2 nsec.

The energy of the incident beam is measured by

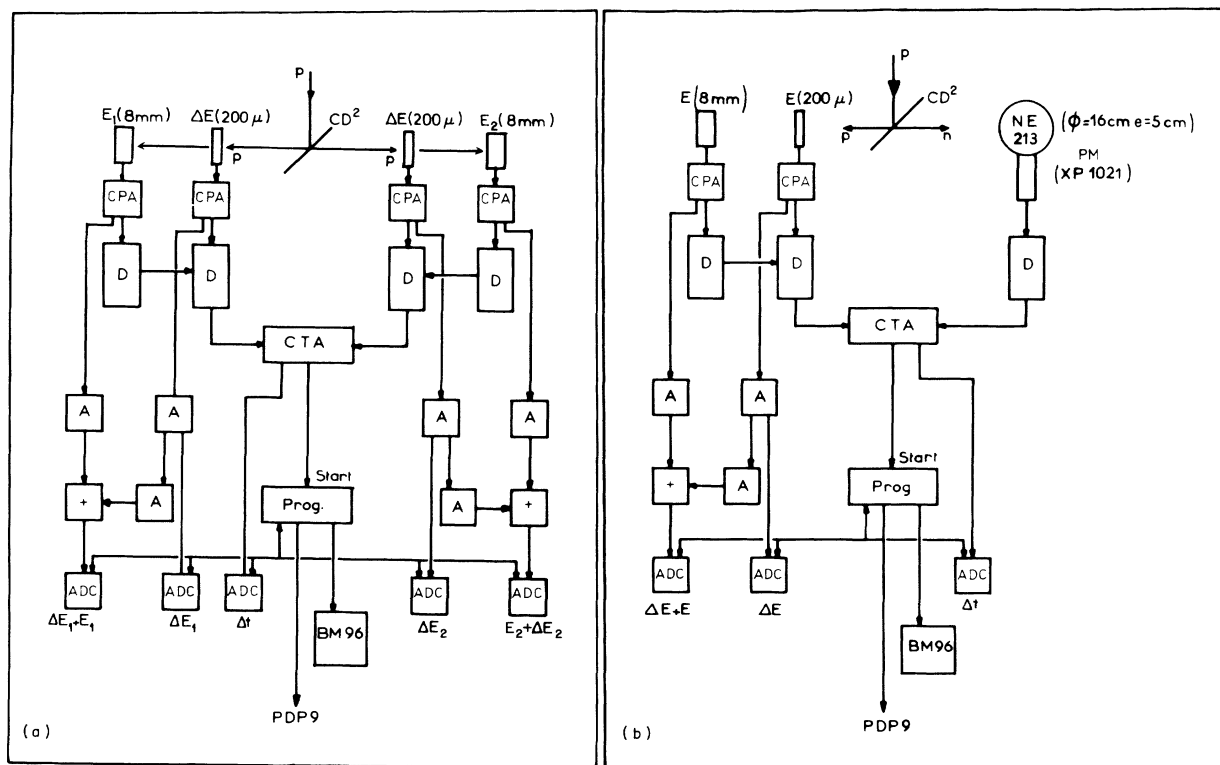


FIG. 1. (a), (b) Simplified electronics system for the  ${}^2\text{H}(p, 2p)$  and  ${}^2\text{H}(p, pn)$  experiments. CPA represents charge preamplifiers, D are discriminators, A are amplifiers, CTA is a time-to-amplitude converter, ADC represents analogic digital converters, and PROG is a program monitor.

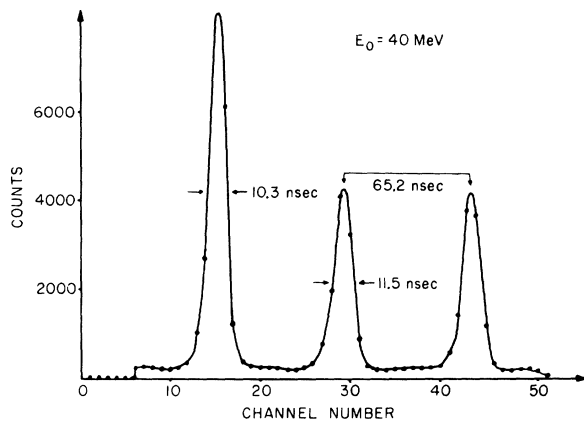


FIG. 2. Typical spectra of time-of-flight difference between the two detected protons in the  ${}^2\text{H}(p, 2p)$  experiment.

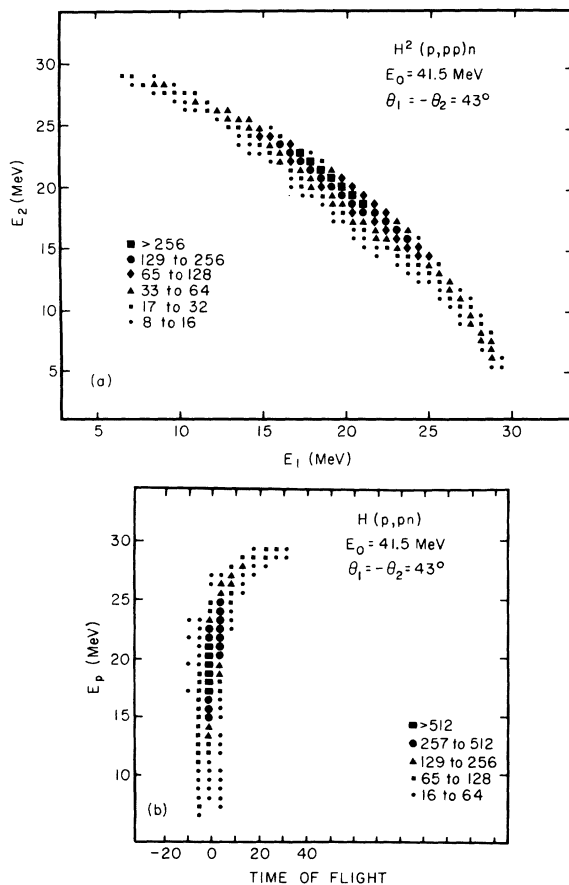


FIG. 3. (a) Typical biparametric display of events in the  $(E_1, E_2)$  plane for the reaction  ${}^2\text{H}(p, p_1 p_2)n$ . The size of a cell is  $0.55 \times 0.60 \text{ MeV}^2$  and the average background is  $=0.1 \text{ events/cell}$ . (b) Typical biparametric display of events in the  $(E_p, \text{TOF})$  plane for the reaction  ${}^2\text{H}(p, np)p$ . The size of a cell is  $0.68 \times 4.6 \text{ MeV nsec}$  and the average background is  $=3.4 \text{ events/cell}$ .

crossover techniques.<sup>13</sup> The free spectrum of one of the proton detectors is stored on a 400-channel analyzer and the absolute calibration of the cross section is given by normalizing the  $p$ - $d$  elastic scattering peak to available data.

### III. EXPERIMENTAL RESULTS

A preliminary account of this work has already been published.<sup>14</sup> Measurements have been done at the following incident energies  $E_0$ : 21.5, 25., 30., 35., 40., 41.5, 49.4, and 56.4 MeV. The triple differential cross section  $\sigma(E_1, \Omega_1, \Omega_2)$  is represented in Fig. 4 as a function of  $E_1$ , the energy of proton 1 detected in the reaction  ${}^2\text{H}(p, p_1 p_2)$  and in Fig. 5, the analog quantity  $\sigma(E_p, \Omega_p, \Omega_n)$  as a function of  $E_p$ , the energy of the proton detected in the reaction  ${}^2\text{H}(p, pn)$ . The error bars are statistical only. The small enhancement appearing sometimes in the high-energy part of the spectra is due to the phase-space factor and/or to the final-state interaction.

Figure 6 gives the variation of  $\sigma(E_1, \Omega_1, \Omega_2)$  at the maximum height of the quasifree peak. The given errors include statistical and absolute normalization uncertainties. The absolute uncertainty is of the order of 10% and is due mainly to uncertainties in the values of the elastic scattering cross sections. In the case of the reaction  ${}^2\text{H}(p, pn)$  the main uncertainty comes from neutron-detection-efficiency measurements. This efficiency has been measured from 2.5 to 14.5 MeV by the hydrogen-scatterer method<sup>15</sup> and a neutron beam produced by the  $\text{T}(d, n)\alpha$  reaction initiated by 200-keV deuterons. The proton threshold was 4.8 MeV. Above 14.5 MeV the efficiency has been extrapolated by using the hypothesis that neutron detection is accomplished only by proton recoils.<sup>16</sup> In fact, this method neglects the possibility of neutron detection by  $n$ - ${}^{12}\text{C}$  interactions. These effects are negligible below 15 MeV and seem to increase with energy,<sup>17</sup> but they are less important when the proton threshold is high. A rough estimate of these possible effects can be obtained by comparing our calculated efficiency for the liquid NE 213 scintillator with direct efficiency measurement by  $n$ - $p$  scattering using an NE 102 plastic scintillator.<sup>18</sup> If these effects are taken into account, the present results should be decreased by a factor of 15% at 40 MeV and 30% at the maximum energy.

The cross sections appear constant as a function of the incident energy in the range 20 to 60 MeV. Our results agree well with preceding measurements done in the same energy range either with the  $(p, 2p)$  reaction<sup>6</sup> or with the  $(p, pn)$  reaction,<sup>4</sup> although the detection angles are sometimes

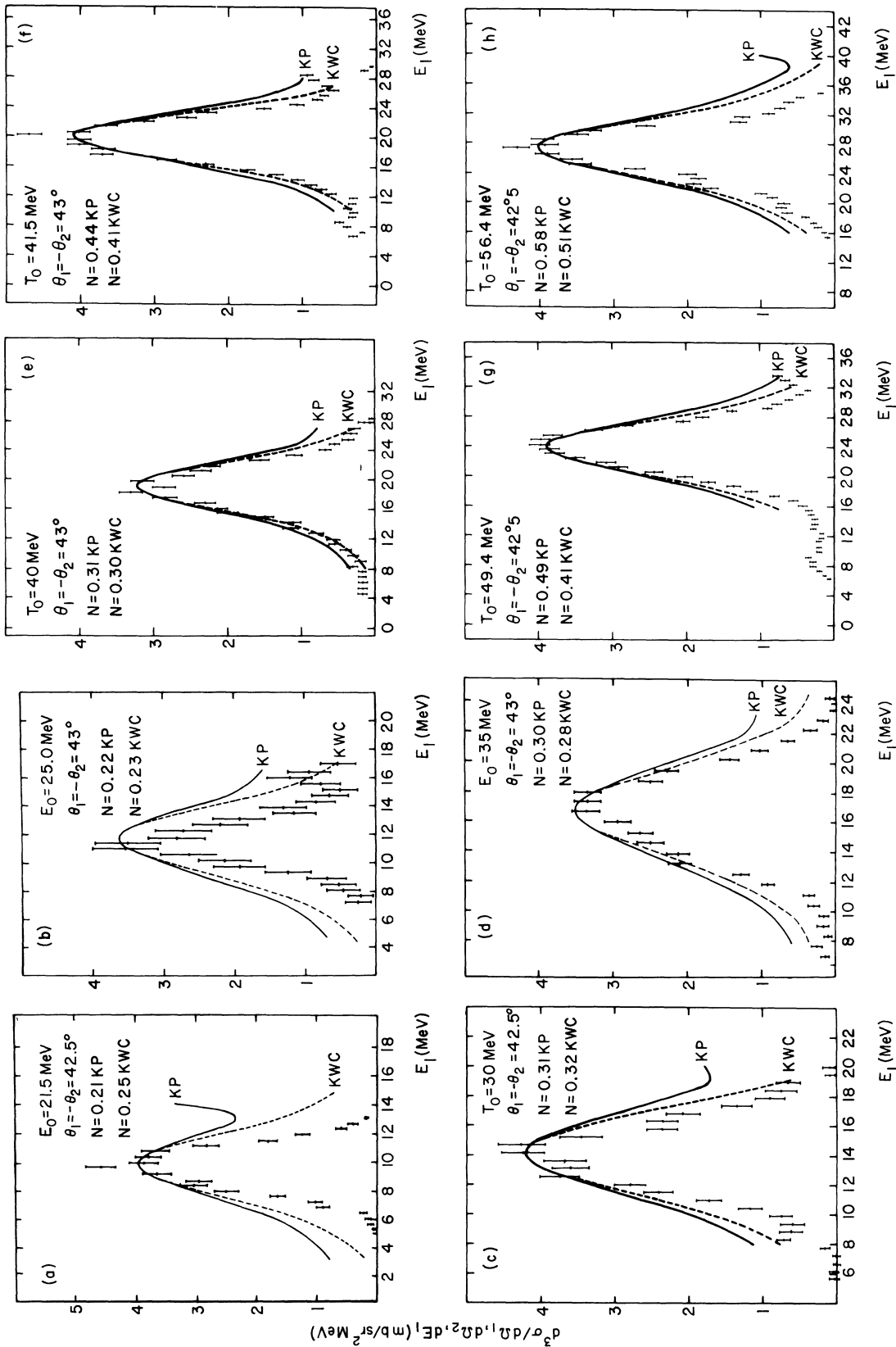


FIG. 4. (a)–(h) Energy spectra of the reaction  ${}^2\text{H}(p_1, p_2)n$ . The solid curves represent the KP calculation normalized to the data. The dashed curves represent the KWC (spectator-model-type) calculation normalized to the data.

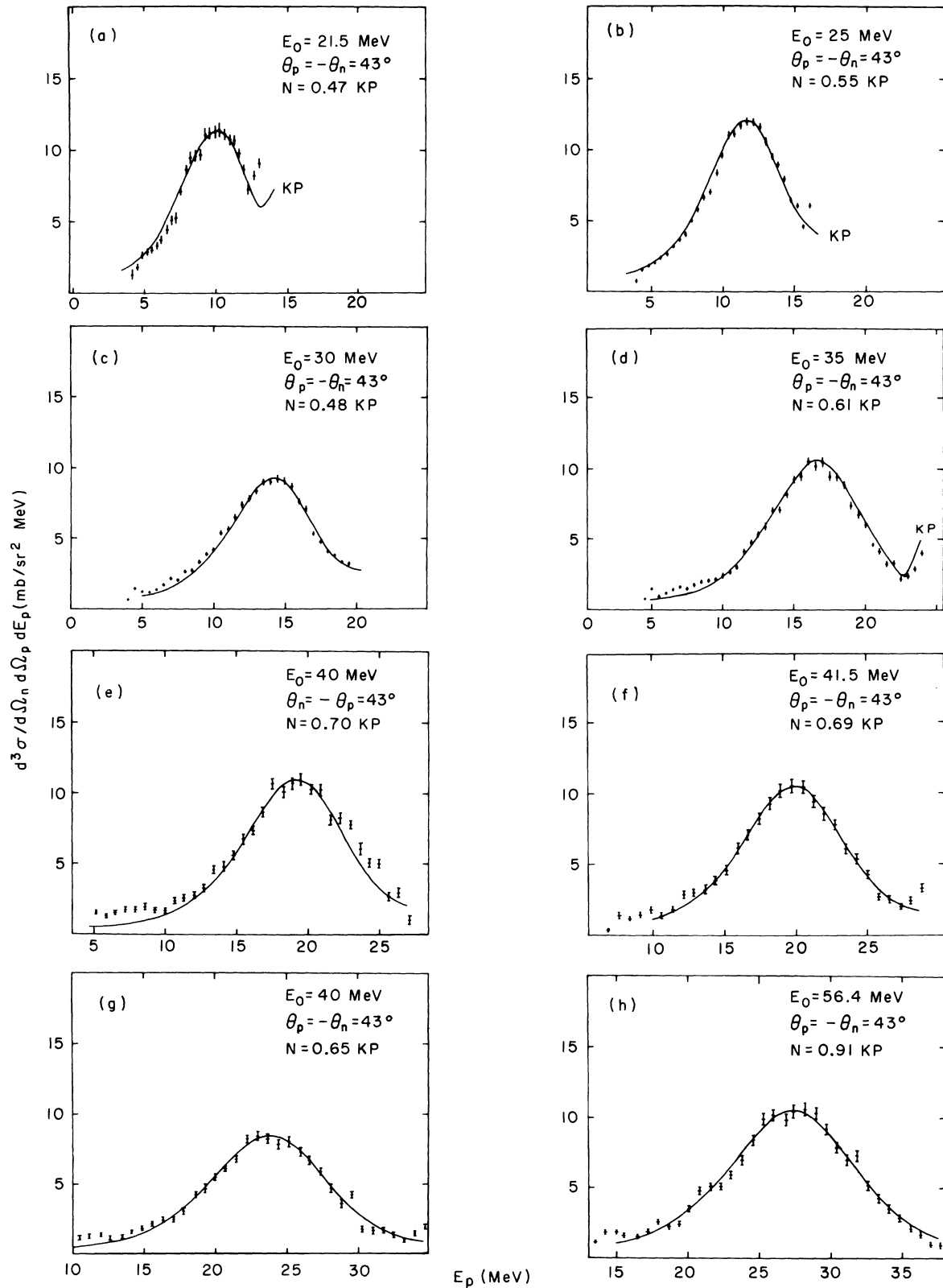


FIG. 5. (a)–(h) Coplanar neutron-proton correlation spectra projected on the proton-energy axis for  $\theta_n = -\theta_p = 43^\circ$ . The solid curves represent the calculation of the simple scattering diagram (KP) normalized to the data.

slightly different. For the  $(p, pn)$  reactions it has been observed<sup>5</sup> that the cross section is also constant at lower energy, although the values quoted in Ref. 5 are higher by a factor 30–40% around  $E_0 = 20$  MeV, where both measurements overlap. A part of this discrepancy is due to a difference in angles of detection.

The  $(p, pn)$  cross section is larger than the  $(p, 2p)$  one by a factor of the order of 2.5; this feature has already been observed at different energies.<sup>2,6</sup> This ratio is larger than the ratio of the free nucleon-nucleon cross sections, especially at low energy.

#### IV. THREE-BODY MODELS

There are many models which have been applied to three-particle interactions. These models have been usually developed to explain some special features of the interaction. For example, the impulse approximation<sup>19</sup> (or spectator model<sup>7</sup>) has been applied for high-energy scattering when the incident particle is supposed to interact with only one particle of the target. With final-state interactions the Migdal-Watson model<sup>20</sup> is particularly suitable. In fact, these models are different approximations of the exact three-body model. The solution of these calculations became numerically possible after the work of Faddeev.<sup>21</sup> The triple

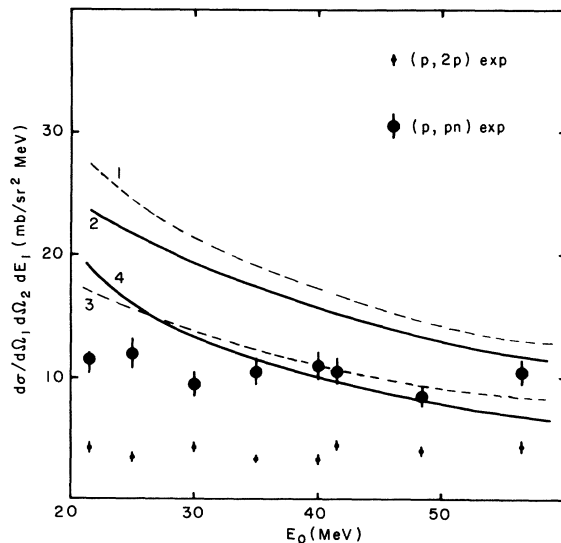


FIG. 6. Energy dependence of the QFS peak cross section for the reactions  ${}^2\text{H}(p, p_1 p_2)n$  and  ${}^2\text{H}(p, np)p$ . The solid curves are the results of the KP calculation [curve 2 shows the  $(p, n)$  QFS and curve 4 that for the  $(p, p)$ ]. The dashed curves are the result of the spectator-model calculations (KWC) [curve 1 shows the  $(p, n)$  QFS and curve 3 that for the  $(p, p)$  QFS].

differential cross section is given by

$$\frac{d^3\sigma}{d\Omega_1 d\Omega_2 dE_1} = \frac{m}{k_0 \hbar^7 (2\pi)^5} \rho |T|^2, \quad (1)$$

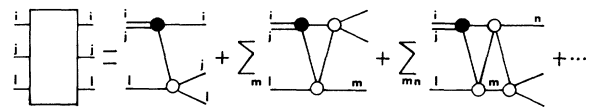
where  $k_0$  and  $m$  are, respectively, the momentum and the mass of the incident particle in the lab system,  $\rho$  is the phase-space density, and  $T = \langle b | T | a \rangle$  is the transition matrix element between the initial and the final state. As a first step the spin effects will be neglected.

The  $T$  matrix is given by the Lippman-Schwinger equation

$$T(z) = V(z) \frac{1}{H_0 - z} T(z), \quad (2)$$

where  $z = E - i\tau$ . This equation cannot be integrated in the general case of an interaction  $V(z)$  between  $n$  particles. On the other hand, if only the two-body interactions are important, Eq. (2) leads to the well-known Faddeev-equation system in which the three-body  $T$  matrix element depends only on two-body  $t$  matrix elements in the three-particle space. Faddeev has shown that these equations have a unique solution independent of the value of  $z$ . The exact solution of the system requires the resolution of three coupled integral equations which cannot yet be calculated even with high-speed modern computers. The problem is simplified when separable nucleon-nucleon potentials are used.<sup>22,23</sup> But in some cases (for example, in the study of elastic nucleon-deuteron scattering below the threshold<sup>24</sup>) more realistic potentials have already been used.

The Faddeev-equation system can alternately be developed as an infinite series of rescattering terms. Each term of the series can be represented by a graph. This formalism is applicable to any three-body reaction no matter what the initial or final states are. In the particular case where the initial state is composed of a proton and a deuteron and the final state by three free nucleons, the amplitude is given by  $\langle k_1 k_2 k_3 | T_i(z) | \varphi_d, k_0 \rangle$ , and the reaction must be represented graphically by Fig. 7. Each term of this series can be considered as an amplitude for a given process. The graphical method has been alternately used (instead of using the Faddeev equations) by Ter-



$$T_i(z) = t_i(z) + \sum_m t_i(z) G_{0m}(z) + \sum_{mn} t_i(z) G_{0m}(z) G_{0n}(z) + \dots$$

FIG. 7. Graphic representation of the  $N + D \rightarrow 3N$  reaction.

TABLE I. Differential cross section  $d^3\sigma/d\Omega_1 d\Omega_2 dE_1$  at the maximum height of the QFS peak for the  ${}^2\text{H}(p, 2p)$  experiment. The indicated error includes statistical and systematic uncertainties.

| Incident energy<br>(MeV) | $d^3\sigma/d\Omega_1 d\Omega_2 dE_1$<br>at the QFS peak<br>(mb/sr <sup>2</sup> MeV) | $N_{\text{KP}}$ | $N_{\text{KWC}}$ | $N_{\text{MDT}_1}$ | $N_{\text{MDT}_{1+2}}$ | $N_{\text{MDT}_{1+2+3}}$ |
|--------------------------|---|-----------------|------------------|--------------------|------------------------|--------------------------|
| 21.5                     | 4.28 ± 0.43   | 0.21            | 0.25             | 0.22               |                        | 0.28                     |
| 25                       | 3.50 ± 0.52   | 0.22            | 0.23             |                    |                        |                          |
| 30                       | 4.30 ± 0.43   | 0.31            | 0.32             |                    |                        |                          |
| 35                       | 3.40 ± 0.51   | 0.30            | 0.28             |                    |                        |                          |
| 40                       | 3.30 ± 0.50   | 0.31            | 0.30             |                    |                        |                          |
| 41.5                     | 4.49 ± 0.45   | 0.44            | 0.41             | 0.48               | 0.90                   | 0.95                     |
| 49.4                     | 3.96 ± 0.40   | 0.49            | 0.41             |                    |                        |                          |
| 56.4                     | 4.39 ± 0.44   | 0.58            | 0.51             | 0.65               | 0.97                   | 1.0                      |

Martirosyan,<sup>25</sup> Komarov and Popova (KP),<sup>26</sup> and Shapiro.<sup>27</sup> When the rescattering series converges rapidly the calculation of the first terms is sufficient and is easier to do than the exact integration of the Faddeev equations. On the other hand in some cases the series diverges (especially at low energy) and this development is no longer justified. So it is very interesting to know the limits of validity of the development as a function of the incident energy. For this purpose our data are compared with different types of calculations: (1) simple spectator model, (2) single-scattering mechanism, and (3) mechanism taking into account rescattering terms up to the third order.

## V. DISCUSSION

### A. Spectator Model (KWC)

The data are compared in Figs. 4 and 5 (dashed line) with the spectator model (KWC),<sup>7</sup> which is the simplest approximation of the single-scattering term. Its characteristics are:

- (1) The incident particle is supposed to interact only with one of the two nucleons of deuteron.
- (2) The free experimental nucleon-nucleon cross section is used instead of the square of the two-

body amplitude. Effects of the spins and the permutation of the particles are not taken into account. Details of this calculation are given, for example, in Ref. 12. We have used the nucleon-nucleon interaction at an energy corresponding to the exit channel. The deuteron wave function is of the Hulthén type<sup>28</sup> in the space representation

$$\varphi(r) = \frac{[2\pi\alpha\beta(\alpha+\beta)]^{1/2}}{2\pi(\beta-\alpha)} \frac{e^{-\alpha r} - e^{-\beta r}}{r}.$$

The calculated values have been normalized to the experimental data; the normalization factors  $N$  are indicated in each figure and are displayed in Table I as a function of the incident energy; for the  $(p, 2p)$  reaction they vary from 0.25 at  $E_0 = 21.5$  MeV to 0.52 at  $E_0 = 56.4$  MeV. For  $n-p$  QFS the normalization factors are displayed in Table II; the agreement is slightly better,  $N$  being equal to 0.41 at 21.5 MeV and 0.84 at 56.4 MeV. These calculations confirm the same type of work done by using a modified simple impulse approximation<sup>6</sup> or MSIA. Concerning the fit of the spectrum shape one sees that the agreement is better at high energy for  $p-p$  QFS. It is good for all the energies for  $n-p$  QFS.

TABLE II. Differential cross section  $d^3\sigma/d\Omega_1 d\Omega_2 dE_1$  at the maximum height of the QFS peak for the  ${}^2\text{H}(p, pn)p$  experiment. The indicated error includes statistical and systematic uncertainties.

| Incident energy<br>(MeV) | $d^3\sigma/d\Omega_1 d\Omega_2 dE_1$<br>at the QFS peak<br>(mb/sr <sup>2</sup> MeV) | $N_{\text{KP}}$ | $N_{\text{KWC}}$ | $N_{\text{MDT}_1}$ | $N_{\text{MDT}_{1+2}}$ | $N_{\text{MDT}_{1+2+3}}$ |
|--------------------------|---|-----------------|------------------|--------------------|------------------------|--------------------------|
| 21.5                     | 11.5 ± 1.4  | 0.47            | 0.41             | 0.55               | 0.19                   | 0.19                     |
| 25                       | 12.0 ± 1.4  | 0.55            | 0.50             |                    |                        |                          |
| 30                       | 9.3 ± 1.1   | 0.48            | 0.42             |                    |                        |                          |
| 35                       | 10.5 ± 1.2  | 0.60            | 0.54             |                    |                        |                          |
| 40                       | 11.0 ± 1.3  | 0.70            | 0.65             |                    |                        |                          |
| 41.5                     | 10.5 ± 1.2  | 0.69            | 0.64             | 0.83               | 0.43                   | 0.5                      |
| 49.4                     | 8.5 ± 1.0   | 0.65            | 0.61             |                    |                        |                          |
| 56.4                     | 10.5 ± 1.2  | 0.91            | 0.84             | 1.25               | 0.85                   | 0.94                     |

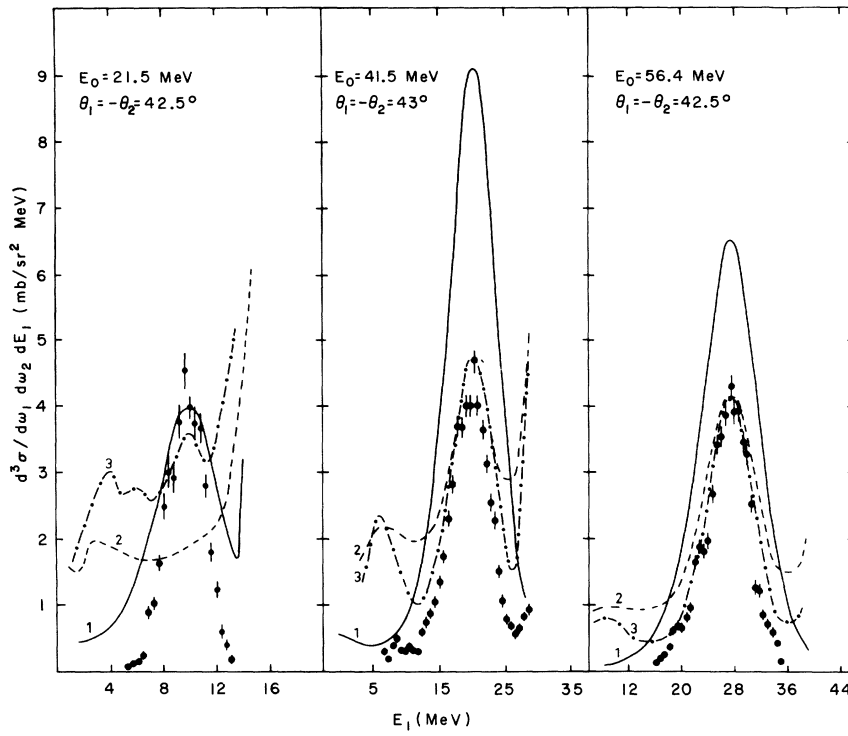


FIG. 8. Coplanar proton-proton correlation spectra projected on the proton 1 energy axis are compared with the MDT calculation. The curves numbered 1 are the result of the simple scattering term calculation. The curves numbered 2 are the result of the calculation of the first two terms of the rescattering series and the curves numbered 3 are the result of the calculation of the first three terms of the rescattering series.

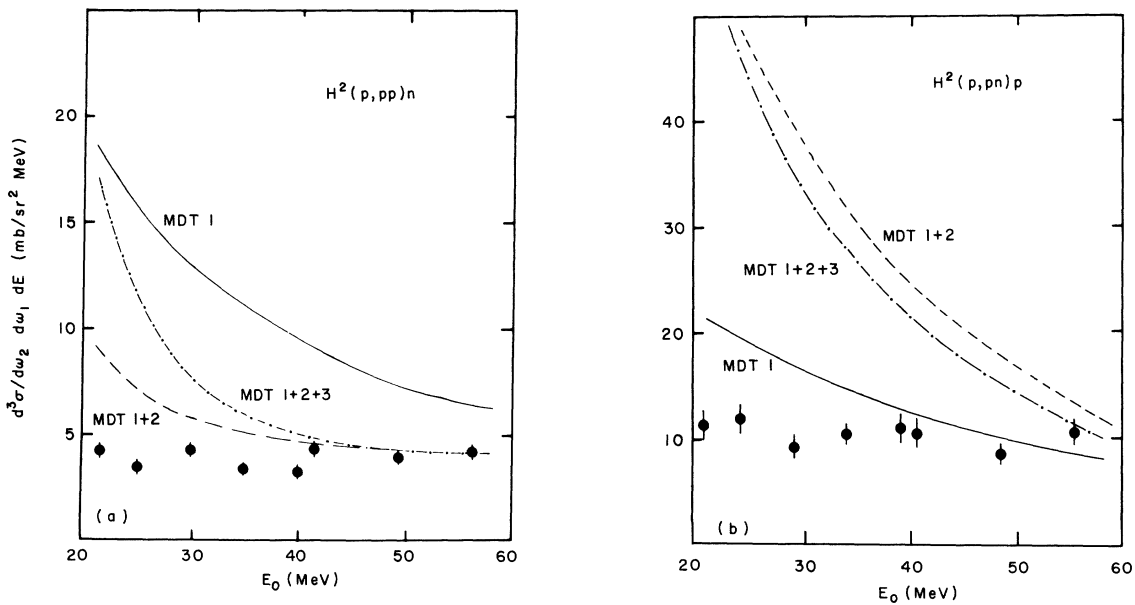


FIG. 9. (a), (b) Energy dependence of the QFS peak cross section for the  ${}^2\text{H}(p, 2p)n$  and  ${}^2\text{H}(p, pn)p$  reactions compared with the MDT calculation.



### B. Single-Scattering Mechanism (KP)

The solid line in Figs. 4 and 5 is the result of a calculation of the first term of the rescattering graph series in which spin and isospin effects have been taken into account following<sup>16,26,29</sup> KP. The transition probability is given by

$$|T|^2 = \frac{2}{3} |T_t^{3/2}|^2 + \frac{1}{3} |T_t^{1/2}|^2 + \frac{1}{3} |T_s^{1/2}|^2.$$

The subscripts  $t$  and  $s$  correspond, respectively, to triplet and singlet nucleon-nucleon interactions; the superscripts  $\frac{1}{2}$  and  $\frac{3}{2}$  correspond to the channel spin of the nucleon-deuteron system. The transition probabilities  $T_t^{3/2}$ ,  $T_t^{1/2}$ , and  $T_s^{1/2}$  are given in Refs. 16 and 29. The Kuckes, Wilson, and Cooper (KWC) calculations are different only in the fact that in the former only the amplitudes corresponding to the two particles in QFS are taken into account. If one compares the two types of calculations, the effect of the permutation of the three particles in the KP calculation is twofold:

- (1) It leaves the absolute value of the  $n$ - $p$  cross section almost unchanged, but the  $p$ - $p$  cross section is increased at low energy and decreased at high energy.
  - (2) It gives broader theoretical spectra, so that the agreement with experiment is worse compared to simple KWC calculations.
- None of these models takes into account off-shell effects.

### C. Calculation of the Rescattering Terms Up to the Third Order (MDT)

The calculations have been performed by one of us (M.D.) by numerical iteration of the Faddeev equations up to the third order. The calculations were first performed with  $s$ -wave separable Yamaguchi potentials,<sup>30</sup> but this potential does not reproduce satisfactorily the nucleon-nucleon cross section above 20 MeV. In an improved version of the calculations, the separable Tabakin potential<sup>31</sup> including  $s$ ,  $p$ , and  $d$  waves with a repulsive core has been used to calculate the first term. In this type of calculation off-shell effects are automatically taken into account. The results are given in Fig. 8 for three different selected energies, namely,  $E_0 = 21.5$ , 41.5, and 56.4 MeV.

#### 1. ( $p, 2p$ ) Calculations

If one looks at the first-order calculations (MDT 1) one sees in Fig. 8 that the results are very close to the KWC and KP calculations which neglect off-shell effects. This is a strong indication that off-shell effects are negligible for first-order calculations at these energies. The same conclusion has been reached when using the Hada-Johnston potential.<sup>32</sup>

At 21.5 MeV the calculations including the rescattering effects up to the third order (MDT 1 + 2 + 3) worsen the fit, which indicates that the

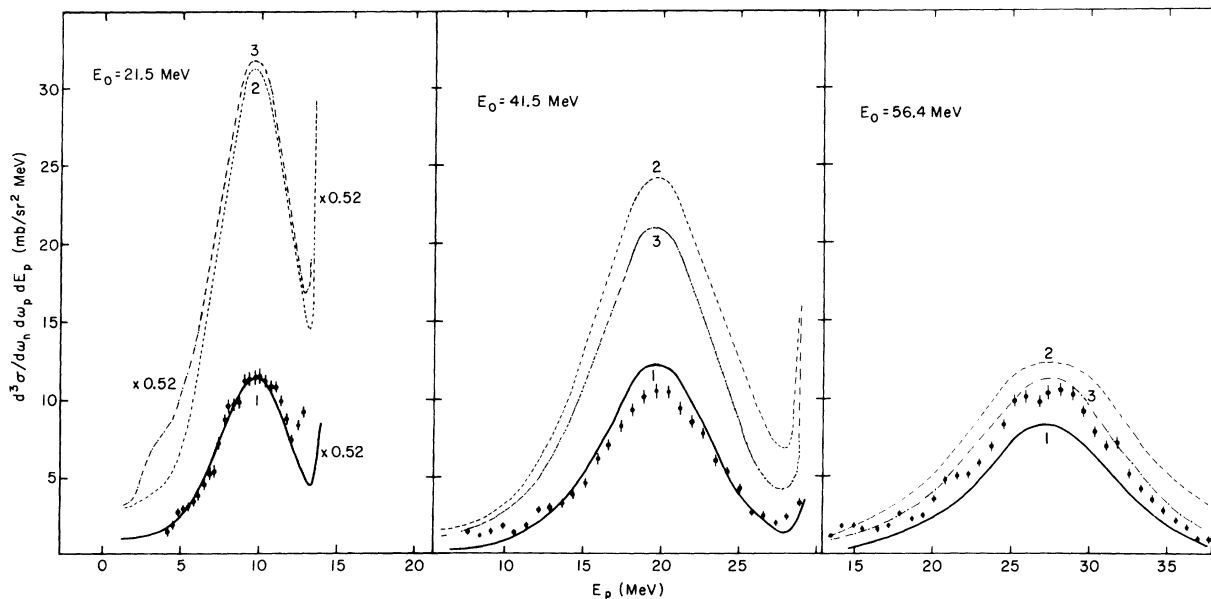


FIG. 10. Coplanar neutron-proton correlation spectra projected on the proton energy axis are compared with the MDT calculation. The curves numbered 1 are the result of the simple scattering term calculation. The curves numbered 2 are the results of the calculation of the first two terms of the rescattering series. The curves numbered 3 are the result of the calculation of the first three terms of the rescattering series.

series does not converge at such a low energy. At 41.5 MeV and 56.4 MeV, taking into account the first two terms (MDT 1 + 2), the calculations converge towards the absolute value of the cross section, but the final-state-interaction effects are enhanced compared to the QFS peak, and the shapes of the spectra are not well reproduced. When the third term is introduced the fit is very good both in magnitude and in shape. These results are displayed as a function of the energy in Fig. 9(a) and Table I.

### 2. ( $p, pn$ ) Calculations

Results are given in Fig. 10. The first-order calculations (MDT 1) give slightly different results than the KWC and KP calculations. This is due mainly to the difference in the way the nucleon-nucleon interaction is introduced. A remarkable feature of these three calculations is that they give absolute values much closer to the experimental ones than in the ( $p, 2p$ ) case. This is due to the fact that the ratio of the ( $p, pn$ ) to ( $p, 2p$ ) cross section is larger than the ratio of the free  $p$ - $n$  to  $p$ - $p$  experimental value. So the normalization factor  $N$  is much closer to unity for ( $p, pn$ ) than ( $p, 2p$ ) QFS.

Second-order calculations give, at all the energies investigated, a value of the cross section higher than that for first-order calculations. This is due to isospin and channel-spin effects peculiar to the  $p$ - $n$  system. But with the introduction of the third rescattering term the calculations con-

verge again towards experimental results, except at 21.5 MeV, where the series diverges. The results as a function of the incident energy are displayed in Table II and Fig. 9(b).

In conclusion, when third-order rescattering effects are taken into account, both ( $p, 2p$ ) and ( $p, pn$ ) calculations converge towards experimental data above 40 MeV for the  ${}^2\text{H}(p, 2p)$  reaction and above 50 MeV for the  ${}^2\text{H}(p, pn)$  reaction.

### VI. CONCLUSION

Single-scattering approximations reproduce quite well the shape of nucleon-nucleon QFS in the breakup of deuterons by protons, but the absolute values are not well fitted. The calculations are in better agreement at high energy than at low energy. The observed discrepancy can be explained either by rescattering effects or by off-shell effects. The importance of rescattering effects has been confirmed experimentally by a measurement of the Treiman-Yang asymmetry<sup>33</sup> in the  $\text{H}(d, 2p)$  reaction at  $E_d = 20$  MeV.

Calculations taking into account both off-shell effects and rescattering effects up to the third order fail to reproduce the experimental data at low energy ( $E_p = 20$  MeV), but are in good agreement both in magnitude and in shape for energies higher than 40 MeV. These results support theoretically the validity of the spectator model at medium energy ( $E_p \geq 100$  MeV), where the number of rescattering terms of order higher than the first become negligible.

<sup>1</sup>A. Niller, C. Joseph, V. Valkovic, W. von Witsch, G. C. Phillips, Phys. Rev. **182**, 1083 (1969).

<sup>2</sup>V. Valkovic, D. Rendic, V. A. Otte, W. von Witsch, G. C. Phillips, Nucl. Phys. **A166**, 547 (1971).

<sup>3</sup>E. L. Petersen, R. G. Allas, R. O. Bondelid, A. G. Pieper, R. B. Theus, Phys. Letters **31B**, 209 (1970).

<sup>4</sup>E. L. Petersen, R. Bondelid, P. Tomas, G. Paic, J. R. Richardson, J. W. Verba, Phys. Rev. **188**, 1497 (1969).

<sup>5</sup>W. J. Braithwaite, J. R. Calarco, J. M. Cameron, D. W. Storm, Nucl. Phys. **A166**, 515 (1971).

<sup>6</sup>D. J. Margaziotis, G. Paic, J. C. Young, J. W. Verba, W. J. Braithwaite, J. M. Cameron, D. W. Storm, T. A. Cahill, Phys. Rev. C **2**, 2050 (1970).

<sup>7</sup>A. F. Kuckes, R. Wilson, P. F. Cooper, Ann. Phys. (N.Y.) **15**, 193 (1961).

<sup>8</sup>M. Morlet, R. Frascaria, B. Geoffrion, N. Marty, B. Tatischeff, A. Willis, Nucl. Phys. **A129**, 177 (1969).

<sup>9</sup>C. N. Brown and E. H. Thorndike, Phys. Rev. **177**, 2067 (1969).

<sup>10</sup>R. T. Cahill and I. H. Sloan, Nucl. Phys. **A165**, 161 (1971).

<sup>11</sup>J. Durisch *et al.*, Nucl. Instr. Methods **80**, 1 (1970).

<sup>12</sup>J. Arvieux, J. L. Durand, J. C. Faivre, D. Garreta, A. Papineau, J. Sura, A. Tarrats, Nucl. Phys. **A150**, 75 (1970).

<sup>13</sup>R. Smythe, Rev. Sci. Instr. **35**, 1197 (1964).

<sup>14</sup>J. L. Durand, J. Arvieux, A. Fiore, and C. Perrin, Phys. Rev. C **4**, 1957 (1971).

<sup>15</sup>R. L. Clarke, Can. J. Phys. **39**, 957 (1961).

<sup>16</sup>J. L. Durand, Ph.D. thesis, Grenoble, 1971 (unpublished).

<sup>17</sup>J. C. Young, J. L. Romero, F. P. Brady, J. R. Morales, Nucl. Instr. Methods **68**, 333 (1969).

<sup>18</sup>F. P. Brady, J. A. Jungerman, J. C. Young, J. L. Romero, P. J. Symonds, Nucl. Instr. Methods **58**, 57 (1968).

<sup>19</sup>G. F. Chew and F. F. Low, Phys. Rev. **113**, 113 (1959).

<sup>20</sup>A. B. Migdal, Zh. Eksperim. i Teor. Fiz. **28**, 3 (1955) [transl.: Soviet Phys. - JETP **1**, 2 (1955)]; K. M. Watson, Phys. Rev. **88**, 1163 (1952).

<sup>21</sup>L. D. Faddeev, Zh. Eksperim. i Teor. Fiz. **39**, 1549 (1960) [transl.: Soviet Phys. - JETP **12**, 1014 (1961)].

<sup>22</sup>R. Aaron, R. D. Amado, and Y. Y. Yam, Phys. Rev. **150**, 857 (1966).

<sup>23</sup>R. T. Cahill and I. H. Sloan, Nucl. Phys. **A165**, 161 (1971).

<sup>24</sup>E. O. Alt and W. Sanhas, private communication.

<sup>25</sup>G. V. Skorniakov and K. A. Ter-Martirosyan, Zh. Eksperim. i Teor. Fiz. **31**, 775 (1956) [transl.: Soviet Phys. - JETP **4**, 648 (1957)].

<sup>26</sup>V. V. Komarov, A. M. Popova, Nucl. Phys. **54**, 278 (1964).

<sup>27</sup>I. S. Shapiro, in *Interaction of High-Energy Particles with Nuclei, Proceedings of the International School of Physics, "Enrico Fermi", Course 38*, edited by T. E. O. Ericson (Academic, N. Y., 1967) p. 220.

<sup>28</sup>L. Hulthen and K. V. Laurikainen, Rev. Mod. Phys. **23**, 1 (1951).

<sup>29</sup>B. Kühn, H. Kumpf, K. Möller, J. Mösner, Nucl.

Phys. **A120**, 285 (1968).

<sup>30</sup>Y. Yamaguchi, Phys. Rev. **95**, 1628 (1954).

<sup>31</sup>F. Tabakin, Ann. Phys. (N.Y.) **30**, 51 (1964).

<sup>32</sup>I. E. MacCarthy and P. C. Tandy, Nucl. Phys. **A178**, 1 (1971).

<sup>33</sup>R. Corfu, J. P. Egger, C. Lunke, C. Nussbaum, J. Rossel, E. Schwarz, J. L. Durand, C. Perrin, Helv. Phys. Acta **43**, 443 (1970).

PHYSICAL REVIEW C

VOLUME 6, NUMBER 2

AUGUST 1972

## Intermediate-State, Single-Particle Energies in Many-Fermion Energy Calculations\*

George A. Baker, Jr.†

*Applied Mathematics Department, Brookhaven National Laboratory, Upton, New York 11973,  
and Baker Laboratory, Cornell University, Ithaca, New York 14850*

and

John L. Gammel

*Los Alamos Scientific Laboratory, Los Alamos, New Mexico 87544*

(Received 17 April 1972)

We show that the naive solution of the two-hole-line-approximation equations for the many-fermion ground-state energy leads to physically incorrect results. As poles cross the integration contour, residue corrections must be appended to the equations. Unfortunately, the corrected equations do not appear to be solvable for nuclear-type potentials.

### 1. INTRODUCTION AND SUMMARY

The purpose of this investigation is to determine the nature of the two-hole-line approximation to the many-fermion energy<sup>1-3</sup> with the Brandow<sup>4</sup> choice for the intermediate-state single-particle energy. Brandow's choice stipulates that the energy for the intermediate-state hole lines be made self-consistent, but that for the filled-state lines remain the unperturbed value. The virtues claimed for this choice are ease of calculation of the hole-line self-energies as compared with those of the filled-state lines, and substantial reduction of the higher-order corrections due to the introduction of a large gap in the single-particle energy spectrum at the Fermi surface for nuclear-type potentials. Yet there is something strange about the procedure, for if instead of a nuclear-type potential we try to apply it to a simple repulsive, square-well potential, the sign of the gap in the single-particle energy spectrum is negative and singularities appear in the integrand of the Green's function, effectively preventing a solution. This whole procedure has been criticized<sup>5</sup> when applied to nuclear-type potentials as either wrong or deceptive. In this paper we will show that the former is in fact the case. The difficulty lies in the motion of the poles of the integrand as we vary the strength of the potential from zero to full.

These poles cross the contour of integration and necessitate residue corrections. The naive method of solution proceeding directly at the full potential without residue corrections leads to an answer which is on the wrong Riemann sheet.

In the second section of this paper we trace the above argument in detail. In the third section we give some numerical calculations to make our conclusions more concrete.

### 2. K MATRIX WITH BRANDOW'S CHOICE FOR THE ENERGY DENOMINATORS

Brandow<sup>4</sup> suggested that one possible treatment for the intermediate-state energy denominators was to make the hole-line energies self-consistent, but not the particle states. This procedure has several seeming advantages and has been used in numerical computations.<sup>6</sup> First, the hole-line energies are always on the energy shell and so readily calculable. Secondly, for potentials of the nuclear type, a large gap at the Fermi surface appears which would seem to cut the magnitude of the correction terms. There is, however, a theoretical problem. In the fourth and higher-order perturbation expansion uncompensated diagrams of the sort shown in Fig. 1 appear. Since all three propagators are the same, there is a third-order singularity in the denominator which can